

Analysis of Techniques for Determining the Number of Electrons Exchanged in Square-Wave Voltammetry



241st ECS Meeting

May 29 - June 2, 2022

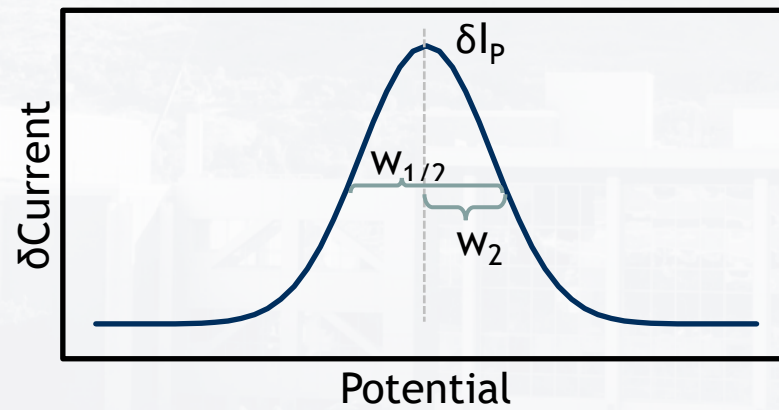
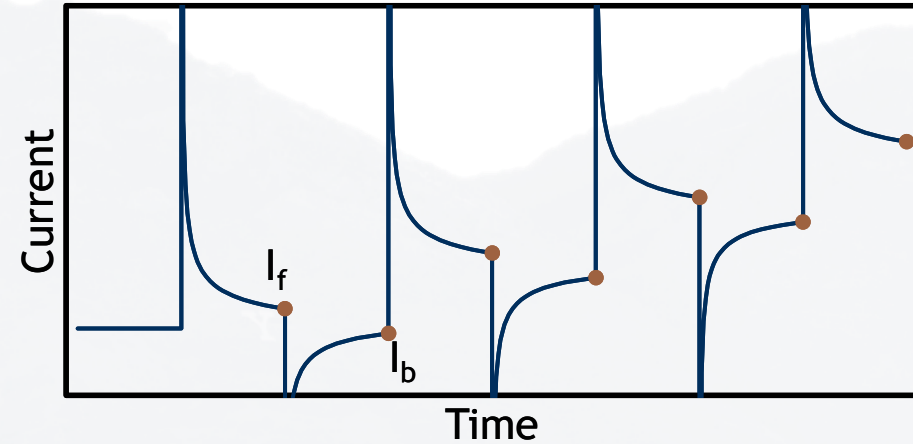
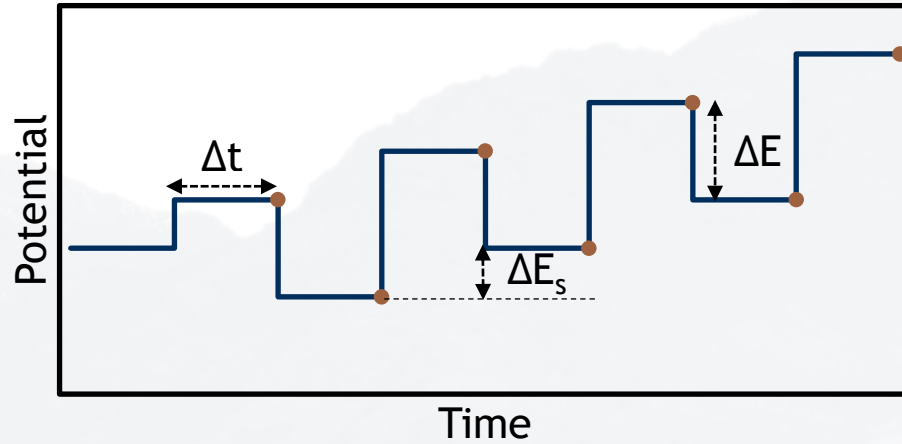
Ranon Fuller, Tyler Williams, Mark Schvaneveldt, Devin Rappleye

Introduction – About me

- PhD Student at Brigham Young University
- Part of the Pyrochemical Research and Operations (PyRO) lab
 - Focus on molten salt chemistry with an emphasis on electrochemical analytical techniques
- My advisor is Devin Rappleye



Introduction – Square-wave voltammetry

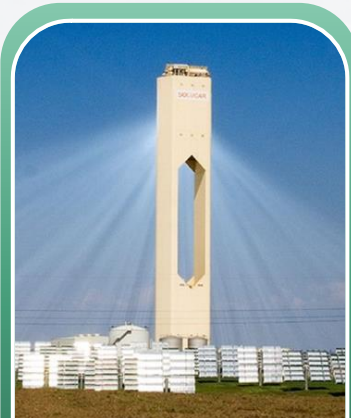


Introduction – Square-wave voltammetry

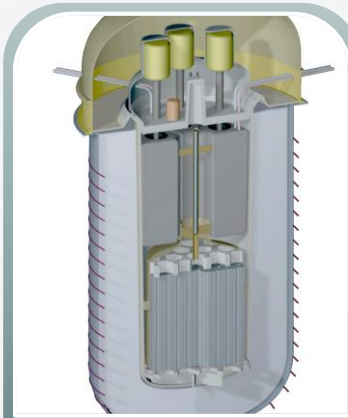
- Square-wave Voltammetry (SWV) can be used to identify the number of electrons exchanged in a redox couple
- Ideal for identifying contaminants in molten salts
- Such applications include:



Nuclear Material
Processing



Solar Power &
Energy Storage



Molten Salt
Reactors



Critical Material
Production



Introduction – Models for calculating n

- Many recent publications have used soluble-soluble reaction models for calculating the number of electrons exchanged (n) in metal deposition²⁻¹¹
 - Since metal deposition is a soluble-insoluble reaction, this application is fundamentally incorrect
- Fatouros and Krulic (2013) noticed this issue and attempted to resolve it by deriving their own SWV model for metal deposition¹²
- We at the PYRO Lab decided to compare the accuracy of each of these models in the cases of aqueous silver deposition and molten salt nickel and lanthanum deposition

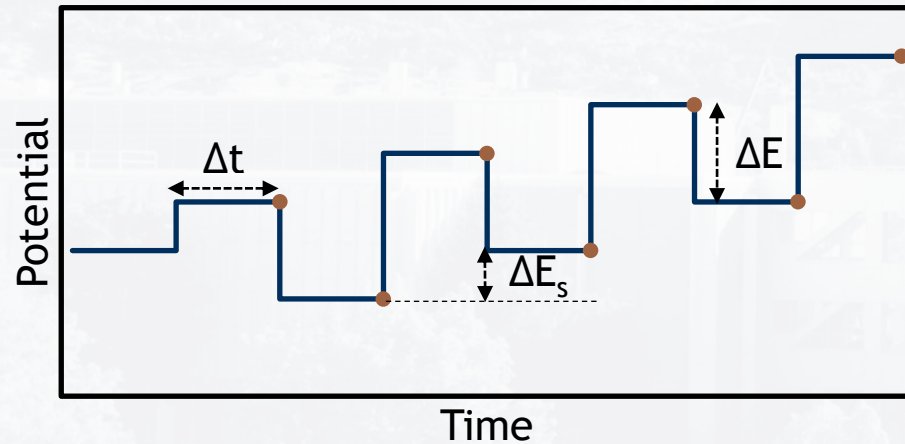


Introduction – Models for calculating n

- Reversible, soluble-soluble reactions:

Barker (1965)¹³

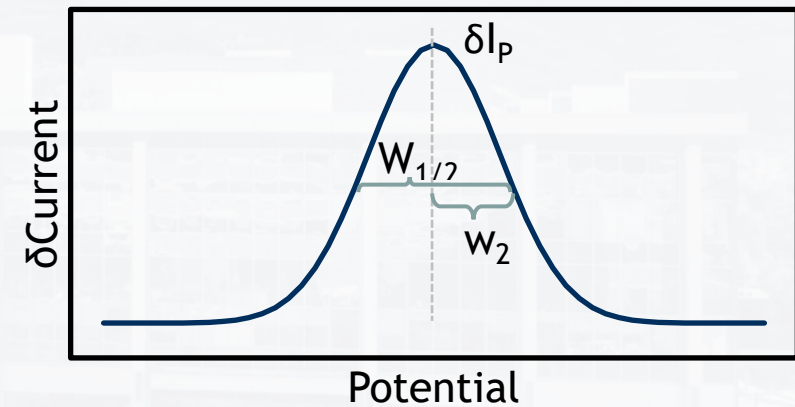
$$W_{1/2} = 3.52 \frac{RT}{nF}$$



Aoki et al. (1986)¹⁴

$$\xi_{SW} = \frac{nF\Delta E}{RT}$$

$$W_{1/2} = \left(\frac{RT}{nF} \right) \left(3.53 + 3.46 \frac{\xi_{SW}^2}{\xi_{SW} + 8.1} \right)$$



Introduction – Models for calculating n

- Reversible, soluble-insoluble reactions:

Fatouros and Krulic (2013)¹²

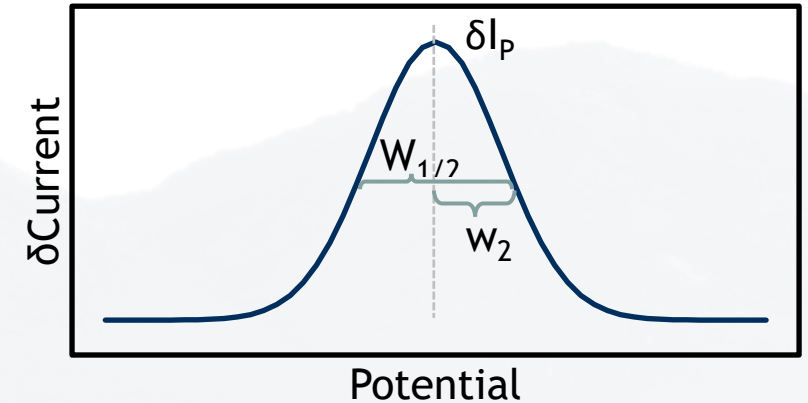
$$w_2 = \frac{W_2 RT}{nF}$$

$$\chi = \frac{C_{ox}^* \sqrt{D_{ox} \Delta t}}{\Gamma_1}$$

$$\rho = \frac{n^2 F^2 A R_u C_{ox}^* \sqrt{D_{ox}}}{RT \sqrt{\Delta t}}$$

- Full model:

$$W_2 = 0.37\chi^{-0.5} + 0.45\chi^{0.11} + (0.26 + 0.01\chi)\rho$$



Introduction – Models for calculating n

- Reversible, soluble-insoluble reactions:

Fatouros and Krulic (2013)¹²

$$w_2 = \frac{W_2 RT}{nF}$$

$$\chi = \frac{C_{ox}^* \sqrt{D_{ox} \Delta t}}{\Gamma_1}$$

$$\rho = \frac{n^2 F^2 A R_u C_{ox}^* \sqrt{D_{ox}}}{RT \sqrt{\Delta t}}$$

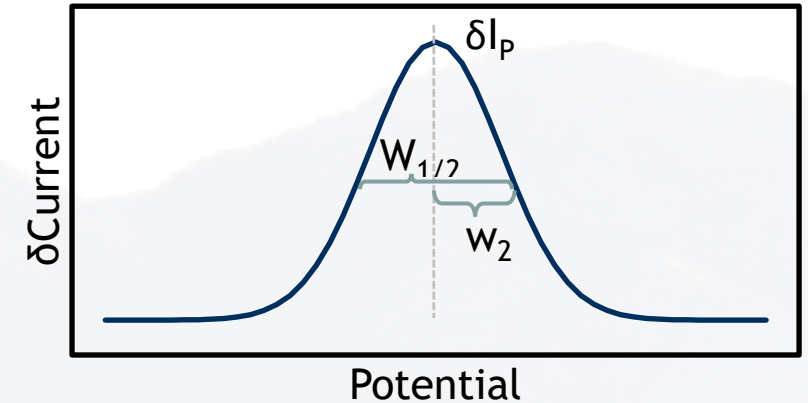
- F&K Truncated (for $\chi > 3.7$):

$$W_2 = 0.7 + 0.3\rho$$

- IR-compensated Fatouros and Krulic model (IR-F&K):

- For Low ρ :

$$W_2 = 0.7$$



Experimental Methods

- Metals tested:

Depositing Metal	Ag ⁺	Ni ²⁺	La ³⁺
Solution	Aqueous HNO ₃	Molten LiCl	Molten LiCl
Working Electrode (WE)	Pt	W	W
Reference Electrode (RE)	Pt-pseudo	W-pseudo	W-pseudo
Counter Electrode (CE)	Pt-coated Nb	W	W
Analyte Concentration	0.027 M	0.419 wt.%	0.433 wt.%
Temperature	23.1°C	701°C	698°C

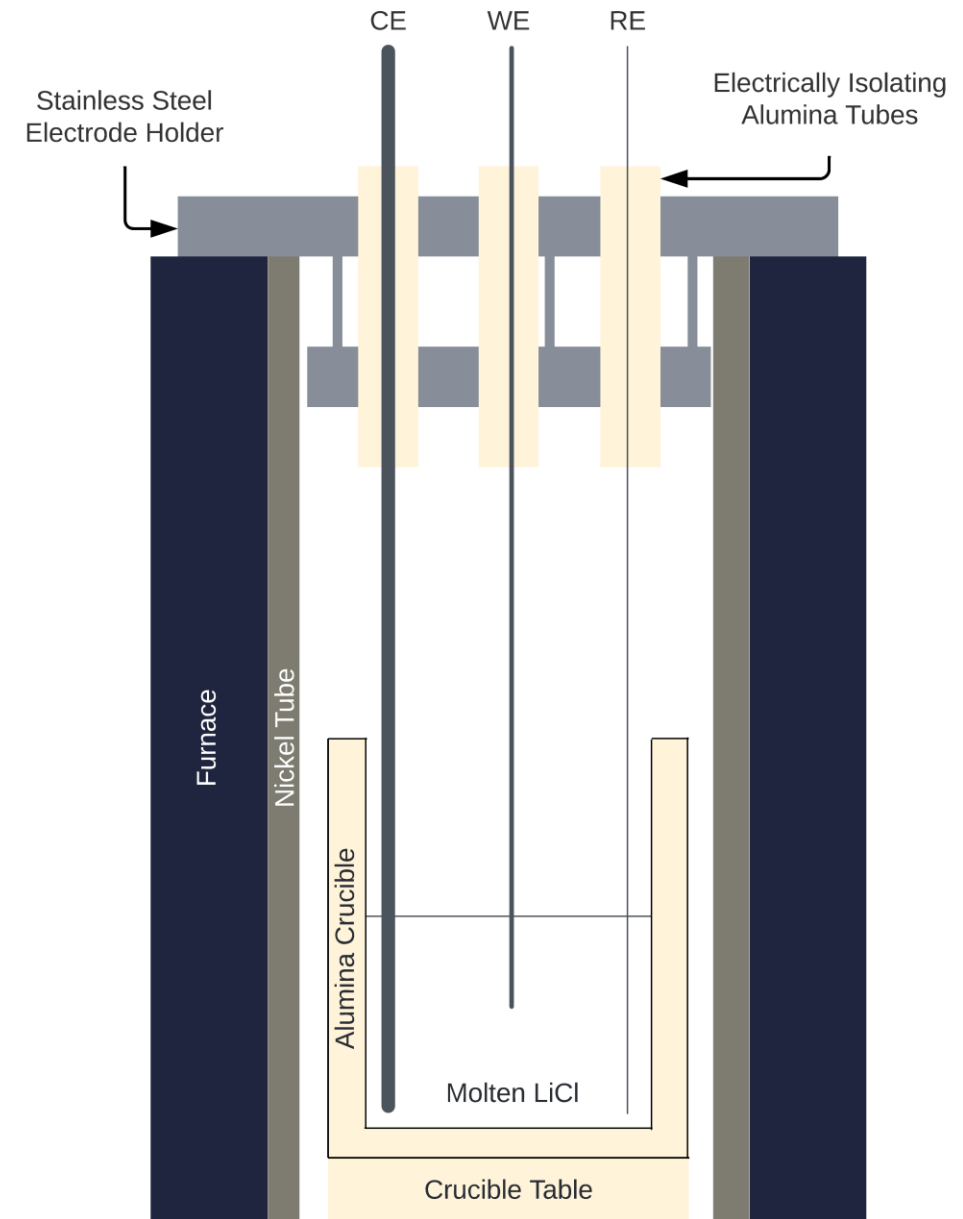


Figure taken from Fuller et al. (2022)¹

Results – Ag deposition on Pt

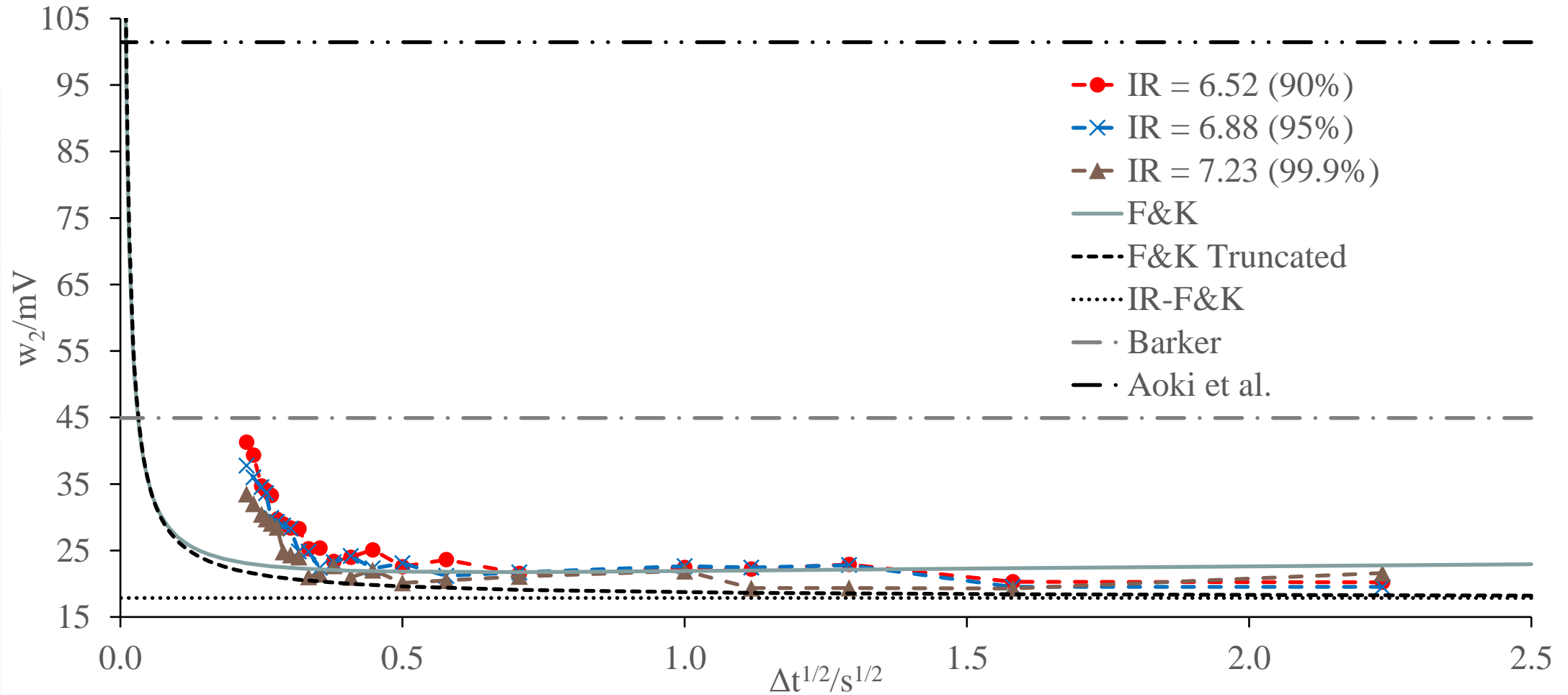


Figure taken from Fuller et al. (2022)¹

Results – Diffusion coefficient of Ni²⁺

- The region of reversibility in cyclic voltammetry was determined via the Berzins-Delahay relationship¹⁵:

$$i_p = 0.6105AC_{ox}^* \sqrt{\frac{(nF)^3 D_{ox} v}{RT}}$$

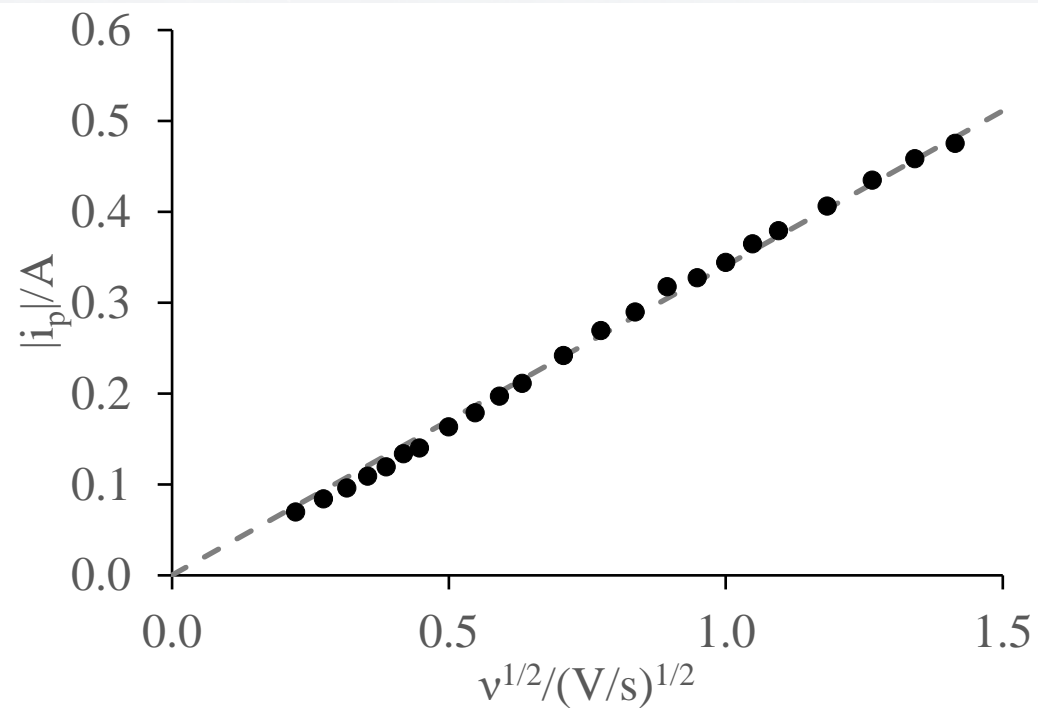


Figure taken from Fuller et al. (2022)¹

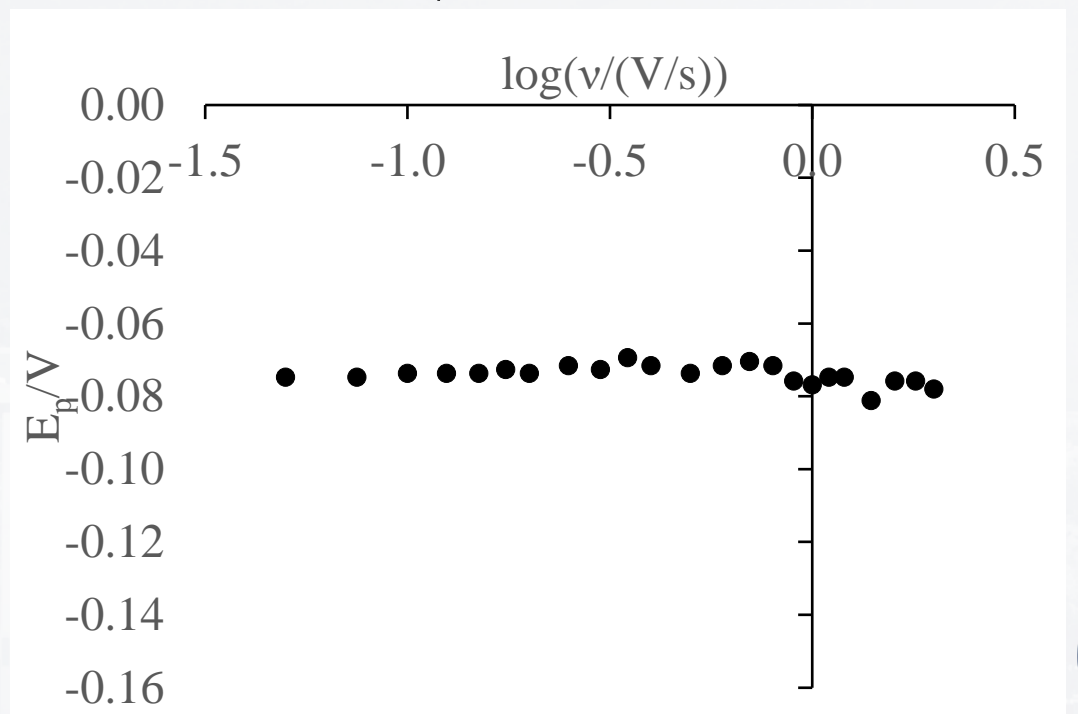


Figure taken from Fuller et al. (2022)¹



Results – Diffusion coefficient of Ni²⁺

- The slope was found to be 0.3408 A s^{1/2}V^{-1/2}
- The concentration of Ni²⁺ in solution was found to be 4.730×10⁻⁵ mol/cm³ as measured by ICP-MS
- $D_{Ni^{2+}} = 3.612 \times 10^{-4} \text{ cm}^2/\text{s}$

$$i_p = 0.6105AC_{ox}^* \sqrt{\frac{(nF)^3 D_{ox} \nu}{RT}}$$

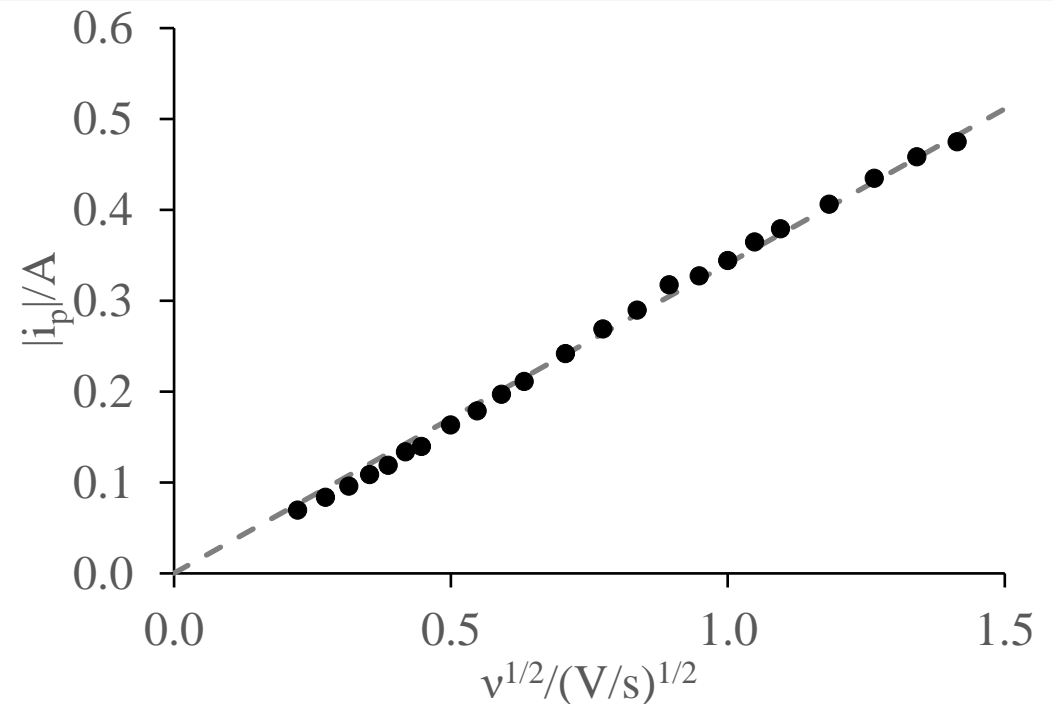


Figure taken from Fuller et al. (2022)¹



Results – Ni deposition on W

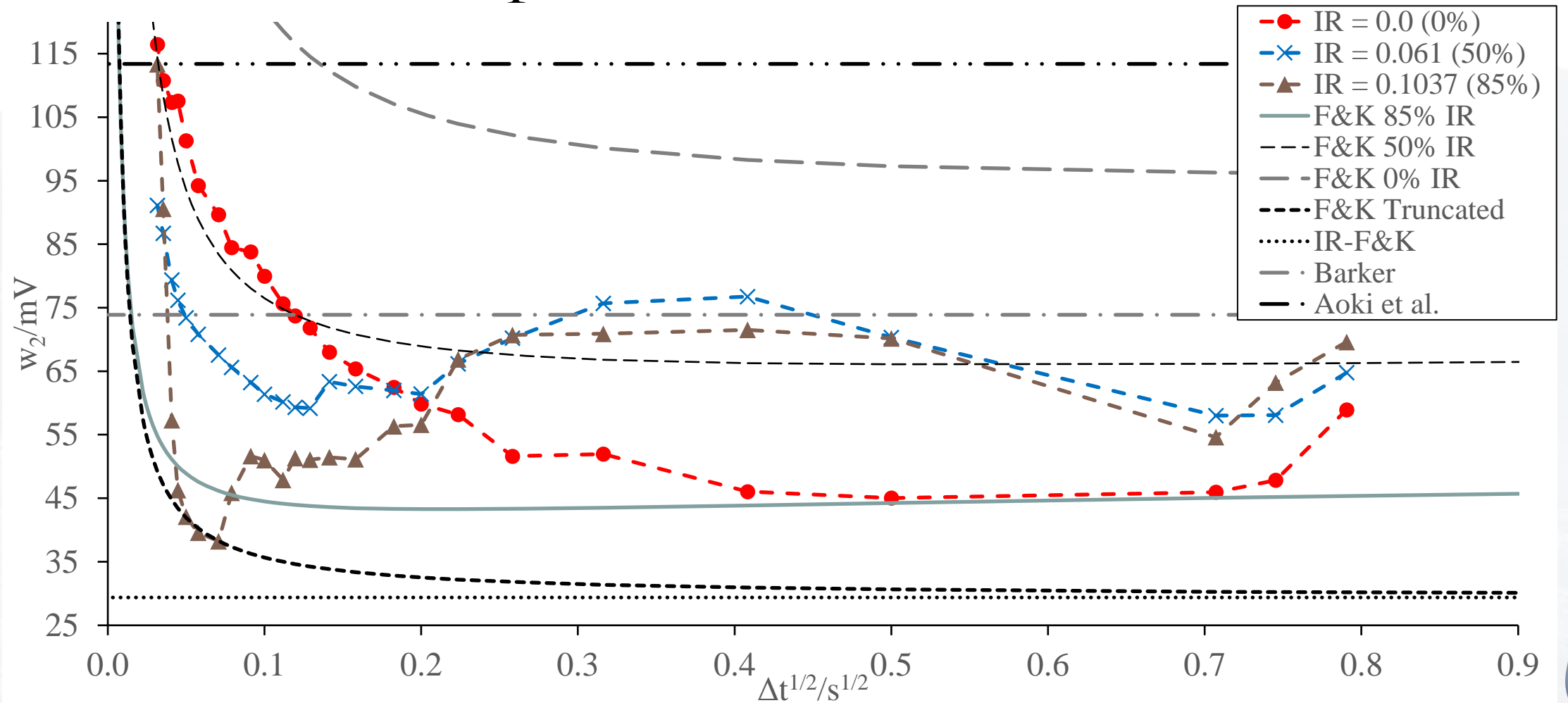


Figure taken from Fuller et al. (2022)¹



Results – Diffusion coefficient of La^{3+}

- The region of reversibility in cyclic voltammetry was determined via the Berzins-Delahay relationship¹⁵:

$$i_p = 0.6105AC_{ox}^* \sqrt{\frac{(nF)^3 D_{ox} v}{RT}}$$

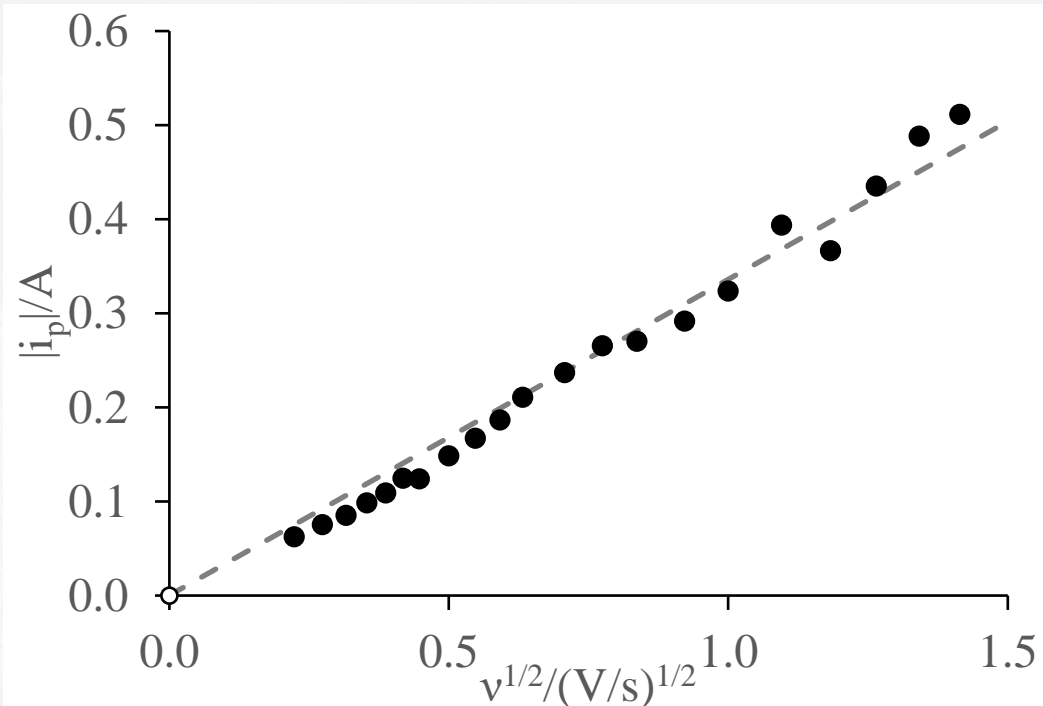


Figure taken from Fuller et al. (2022)¹

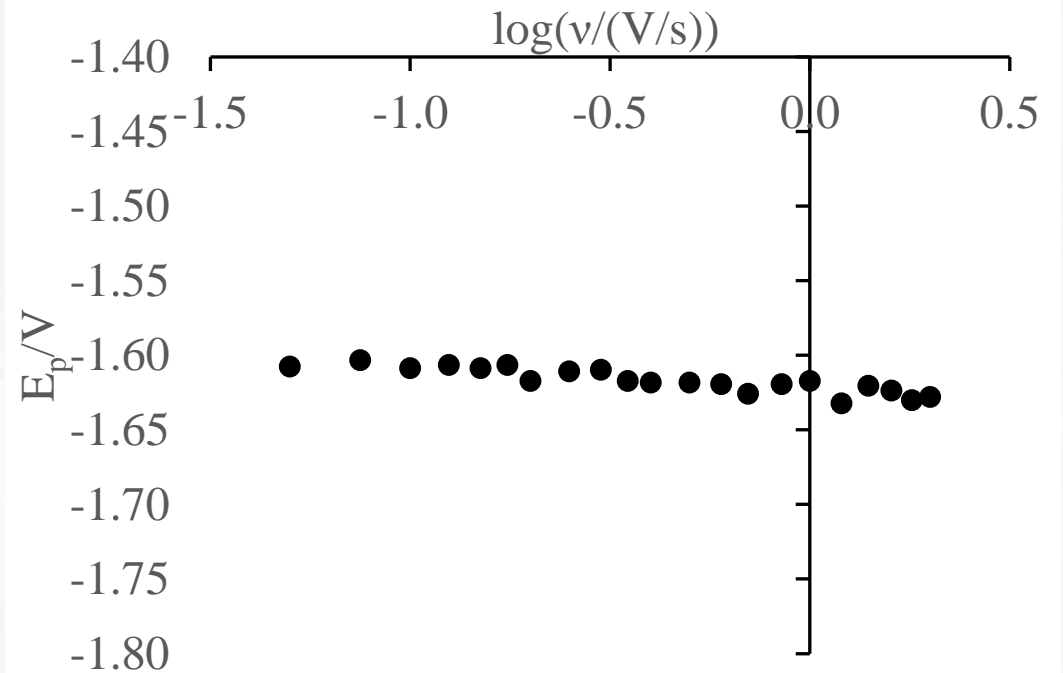


Figure taken from Fuller et al. (2022)¹



Results – Diffusion coefficient of La^{3+}

- The slope was found to be $0.3358 \text{ A s}^{1/2}\text{V}^{-1/2}$
- The concentration of La^{3+} in solution was found to be $2.586 \times 10^{-5} \text{ mol/cm}^3$ as measured by ICP-MS
- $D_{\text{La}^{3+}} = 3.42 \times 10^{-4} \text{ cm}^2/\text{s}$

$$i_p = 0.6105 A C_{ox}^* \sqrt{\frac{(nF)^3 D_{ox} \nu}{RT}}$$

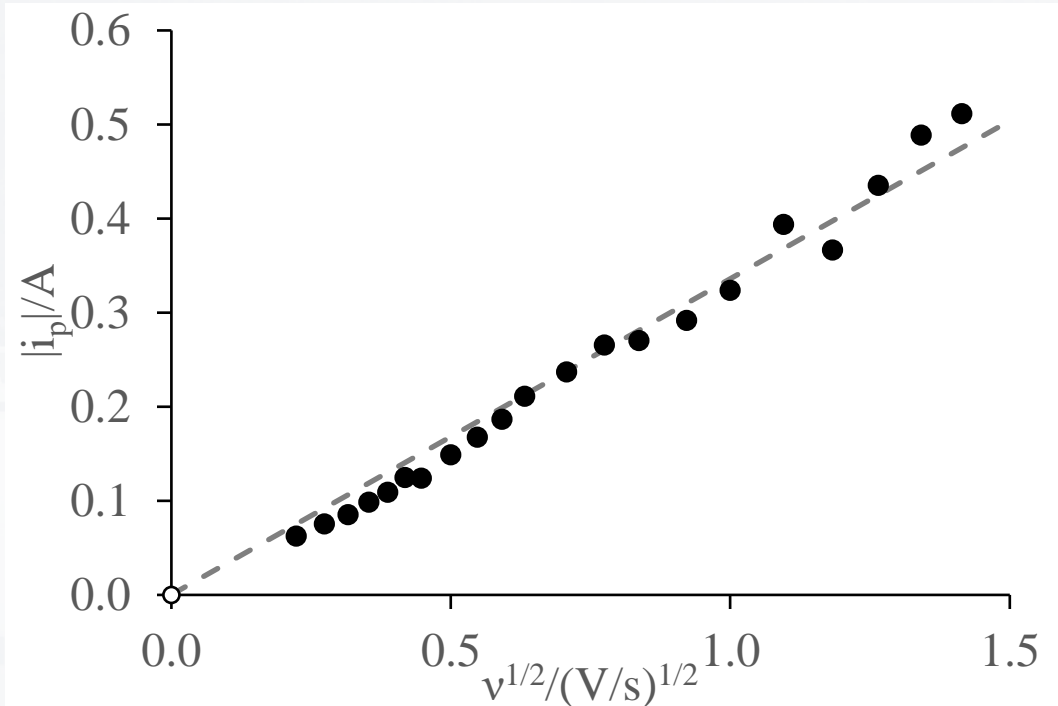


Figure taken from Fuller et al. (2022)¹



Results – La deposition on W

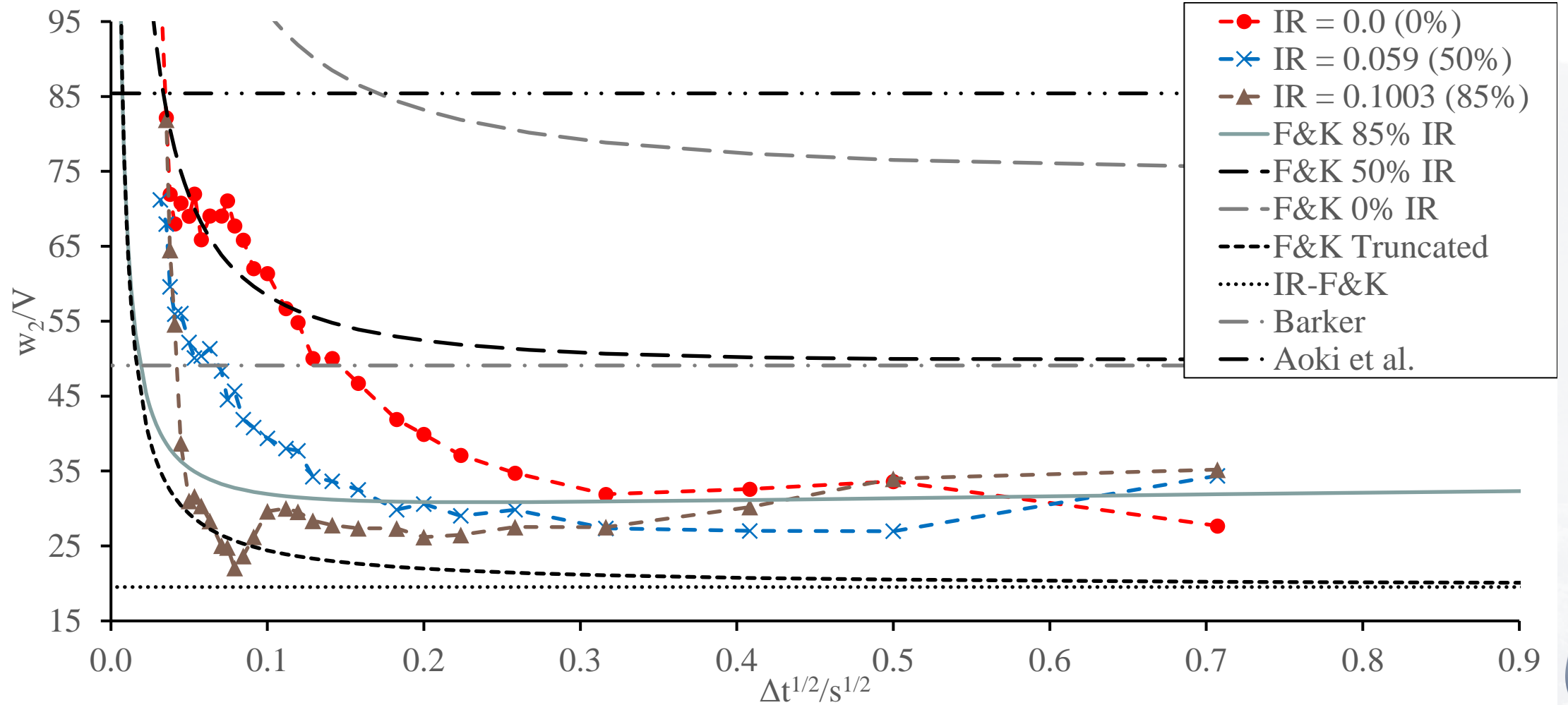


Figure taken from Fuller et al. (2022)¹



Comparison of models for calculating n

Trial	Barker		Aoki et al.		F&K		F&K Truncated		IR-F&K	
	n	Error	n	Error	n	Error	n	Error	n	Error
Ag 90%	2.22	122%	1.14	14%	1.48	48%	0.92	8%	0.88	12%
Ni 85%	2.89	45%	3.74	87%	1.50	25%	1.21	40%	1.15	43%
La 85%	5.39	80%	4.66	55%	4.54	51%	2.32	23%	2.15	28%

Table adapted from Fuller et al. (2022)¹



Limits of full Fatouros and Krulic model

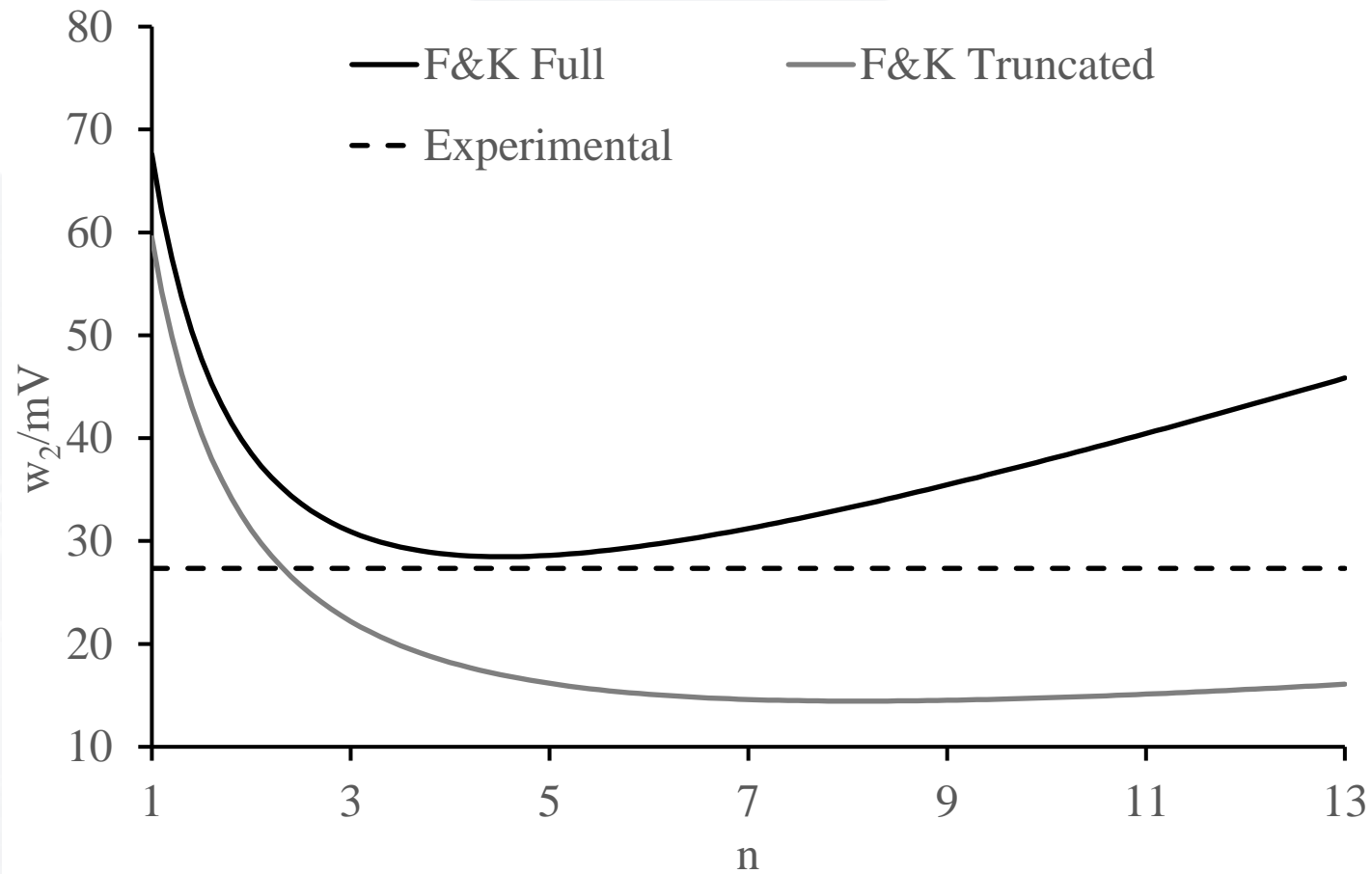


Figure taken from Fuller et al. (2022)¹



Alternative linear fit

- New, experimentally observed linear fit

$$W_2 = 0.91 + 0.32\rho$$

- In the well-compensated case, this would simplify to:

$$W_2 = 0.91$$

- Using this to calculate n results in:
 - $n = 1.06$ for Ag deposition at 90% IR compensation
 - $n = 1.49$ for Ni deposition at 85% IR compensation
 - $n = 2.79$ for La deposition at 85% IR compensation



Conclusion

- Soluble-soluble models are not consistently accurate for determining the number of electrons exchanged in metal deposition
- The IR-compensated Fatouros and Krulic model can be used to reliably predict the correct number of electrons exchanged for one, two, and three electron exchange, metal deposition reactions
- We suggest this method be used for rapid determination of n where concentrations and diffusion coefficients may be unknown



References

1. R. Fuller, A comparison of square-wave voltammetry models to determine the number of electrons exchanged in metal deposition, *Electrochimica Acta*. (2022) 11. <https://doi.org/10.1016/j.electacta.2022.140220>
2. M.R. Bermejo, E. Barrado, A.M. Martínez, Y. Castrillejo, Electrodeposition of Lu on W and Al electrodes: Electrochemical formation of Lu-Al alloys and oxoacidity reactions of Lu(III) in the eutectic LiCl-KCl, *J. Electroanal. Chem.* 617 (2008) 85-100. <https://doi.org/10.1016/j.jelechem.2008.01.017>.
3. M.R. Bermejo, J. Gómez, A.M. Martínez, E. Barrado, Y. Castrillejo, Electrochemistry of terbium in the eutectic LiCl-KCl, *Electrochimica Acta*. 53 (2008) 5106-5112. <https://doi.org/10.1016/j.electacta.2008.02.058>.
4. S. Ghosh, S. Vandarkuzhali, P. Venkatesh, G. Seenivasan, T. Subramanian, B. Prabhakara Reddy, K. Nagarajan, Electrochemical studies on the redox behaviour of zirconium in molten LiCl-KCl eutectic, *J. Electroanal. Chem.* 627 (2009) 15-27. <https://doi.org/10.1016/j.jelechem.2008.12.011>.
5. C. Hamel, P. Chamelot, P. Taxil, Neodymium(III) cathodic processes in molten fluorides, *Electrochimica Acta*. 49 (2004) 4467-4476. <https://doi.org/10.1016/j.electacta.2004.05.003>.
6. C. Hamel, P. Chamelot, A. Laplace, E. Walle, O. Dugne, P. Taxil, Reduction process of uranium(IV) and uranium(III) in molten fluorides, *Electrochimica Acta*. 52 (2007) 3995-4003. <https://doi.org/10.1016/j.electacta.2006.11.018>.
7. K. Serrano, P. Taxil, Electrochemical reduction of trivalent uranium ions in molten chlorides, (n.d.) 7.
8. J. Serp, P. Chamelot, S. Fourcaudot, R.J.M. Konings, R. Malmbeck, C. Pernel, J.C. Poignet, J. Rebizant, J.-P. Glatz, Electrochemical behaviour of americium ions in LiCl-KCl eutectic melt, *Electrochimica Acta*. 51 (2006) 4024-4032. <https://doi.org/10.1016/j.electacta.2005.11.016>.
9. P. Chamelot, B. Lafage, P. Taxil, Using square-wave voltammetry to monitor molten alkaline fluoride baths for electrodeposition of niobium, *Electrochimica Acta*. 43 (1998) 607-616. [https://doi.org/10.1016/S0013-4686\(97\)00102-3](https://doi.org/10.1016/S0013-4686(97)00102-3).
10. P. Chamelot, P. Taxil, B. Lafage, Voltammetric studies of tantalum electrodeposition baths, *Electrochimica Acta*. 39 (1994) 2571-2575. [https://doi.org/10.1016/0013-4686\(94\)00262-2](https://doi.org/10.1016/0013-4686(94)00262-2).
11. Y. Castrillejo, M.R. Bermejo, A.M. Martínez, A. Díaz, Electrochemical behavior of lanthanum and yttrium ions in two molten chlorides with different oxoacidic properties: The eutectic LiCl-KCl and the equimolar mixture CaCl₂-NaCl, *J. Min. Metall. Sect. B Metall.* 39 (2003) 109-135. <https://doi.org/10.2298/JMMB0302109C>.
12. N. Fatouros, D. Krulic, Analysis of the square wave voltammetry for reversible metal deposition on a foreign substrate - Experimental study of silver deposition on gold, *J. Electroanal. Chem.* 706 (2013) 76-85. <https://doi.org/10.1016/j.jelechem.2013.07.019>.
13. G.C. Barker, R.L. Faircloth, A.W. Gardner, Square wave polarography. Part IV. An introduction to the theoretical aspects of square wave polarography, (1956). <https://www.osti.gov/biblio/4317989>.
14. K. Aoki, K. Tokuda, H. Matsuda, J. Osteryoung, Reversible square-wave voltammograms independence of electrode geometry, *J. Electroanal. Chem. Interfacial Electrochem.* 207 (1986) 25-39. [https://doi.org/10.1016/0022-0728\(86\)87060-7](https://doi.org/10.1016/0022-0728(86)87060-7).
15. T. Berzins, P. Delahay, Oscillographic Polarographic Waves for the Reversible Deposition of Metals on Solid Electrodes, *J. Am. Chem. Soc.* 75 (1953) 555-559. <https://doi.org/10.1021/ja01099a013>.



Questions?



Methods – Ag deposition on Pt

- Three sets of SVW measurements were performed at different IR compensations:
 - 90% compensation (6.52 Ω)
 - 95% compensation (6.88 Ω)
 - 99.9% compensation (7.23 Ω)

Table 1: Experimental parameters compared to the range recommended by Fatouros and Krulic

	$\Delta E_s/V$	$\Delta E/V$
Recommended Range	-0.0059 to -0.0010	0.020 to 0.120
Experimental Parameters	-0.003	0.1

Table adapted from Fuller et al. (2022)¹



Results – Ag deposition on Pt

Table 2: Representative w_2 and their associated χ values for silver deposition on platinum in aqueous HNO_3

	$\Delta t^{1/2} / s^{1/2}$	f / Hz	w_2 / V	χ
IR = 6.52 Ω (90%)	2.24	0.1	0.0202	142
IR = 6.88 Ω (95%)	2.24	0.1	0.0195	142
IR = 7.23 Ω (99.9%)	1.58	0.2	0.0193	101

Table adapted from Fuller et al. (2022)¹



Methods – Ni deposition on W

- Diffusion coefficients were calculated by the relationship derived by Berzins and Delahay (1953)
 - For a reversible soluble-insoluble reaction:

$$i_p = 0.6105AC_{ox}^* \sqrt{\frac{(nF)^3 D_{ox} \nu}{RT}}$$

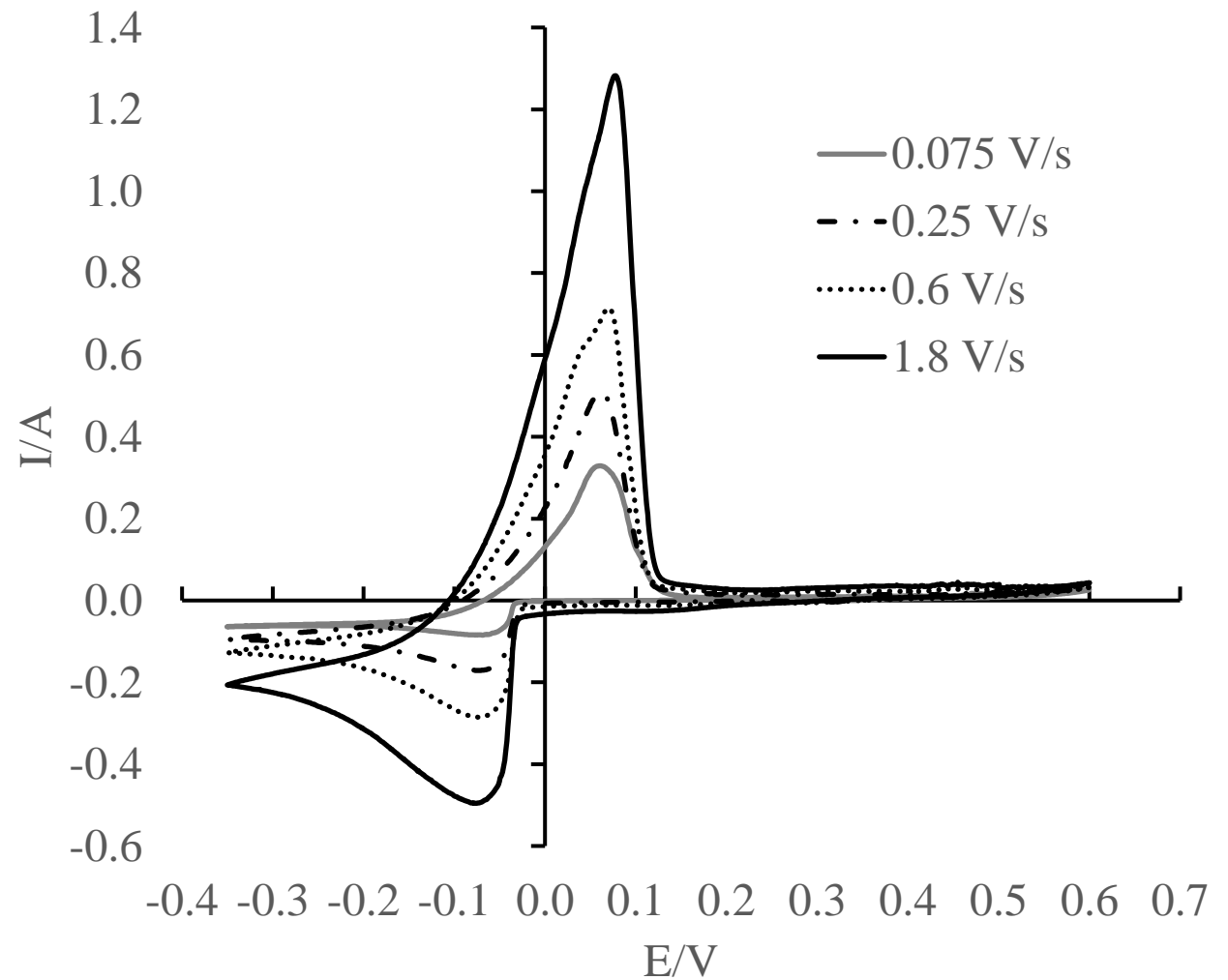


Figure taken from Fuller et al. (2022)¹

Methods – Ni deposition on W

- SWV measurements were conducted at a range of frequencies and IR compensations:
 - 0.0% compensation
 - 50% compensation (0.061 Ω)
 - 85% compensation (0.1037 Ω)

Table 3: Experimental and recommended parameters for Ni deposition on W

	$\Delta E_s/V$	$\Delta E/V$
Recommended Range [13]	-0.00965 to -0.00168	0.034 to 0.197
Experimental Parameters	-0.005	0.1

Table adapted from Fuller et al. (2022)¹



Results – Ni deposition on W

Table 4: Representative w_2 and their associated χ values for nickel deposition on tungsten in molten LiCl

	$\Delta t^{1/2} / \text{s}^{1/2}$	f / Hz	w_2 / V	χ
IR = 0.0 Ω (0%)	0.158	20	0.0654	62.4
IR = 0.061 Ω (50%)	0.129	30	0.0592	50.9
IR = 0.1037 Ω (85%)	0.158	20	0.0511	62.4

Table adapted from Fuller et al. (2022)¹



Methods – La deposition on W

- SWV measurements were conducted at a range of frequencies and IR compensations:
 - 0.0% compensation
 - 50% compensation (0.059 Ω)
 - 85% compensation (0.1003 Ω)

Table 5: Experimental and recommended parameters for La deposition on W

	$\Delta E_s/V$	$\Delta E/V$
Recommended Range [13]	-0.00642 to -0.00112	0.022 to 0.131
Experimental Parameters	-0.003	0.08

Table adapted from Fuller et al. (2022)¹



Results – La deposition on W

Table 6: Representative w_2 and their associated χ values for Lanthanum deposition on tungsten in molten LiCl

	$\Delta t^{1/2} / \text{s}^{1/2}$	f / Hz	w_2 / V	χ
IR = 0.0 Ω (0%)	0.183	15	0.0419	79.9
IR = 0.059 Ω (50%)	0.183	15	0.0299	79.9
IR = 0.1003 Ω (85%)	0.183	15	0.0273	79.9

Table adapted from Fuller et al. (2022)¹



Comparison of models for calculating n

Trial	Barker		Aoki et al.		F&K		F&K Truncated		IR-F&K	
	n	Error	n	Error	n	Error	n	Error	n	Error
Ag 90%	2.22	122%	1.14	14%	1.48	48%	0.92	8%	0.88	12%
Ag 95%	2.30	130%	1.14	14%	1.22	22%	0.93	7%	0.92	8%
Ag 99%	2.33	133%	1.14	14%	1.04	4%	0.93	7%	0.93	7%
Ni 0%	2.26	13%	3.74	87%	1.27	37%	1.18	41%	0.90	55%
Ni 50%	2.50	25%	3.74	87%	1.73	13%	1.19	41%	0.99	50%
Ni 85%	2.89	45%	3.74	87%	1.50	25%	1.21	40%	1.15	43%
La 0%	3.52	17%	4.64	55%	1.75	42%	1.91	36%	1.40	53%
La 50%	4.93	64%	4.75	58%	2.48	17%	2.66	11%	1.96	35%
La 85%	5.39	80%	4.66	55%	4.54	51%	2.32	23%	2.15	28%

Table adapted from Fuller et al. (2022)¹

